Chemical Engineering and Processing 82 (2014) 112–122

Contents lists available at ScienceDirect

Chemical Engineering and Processing: Process Intensification

journal homepage: www.elsevier.com/locate/cep

Optimal design of cryogenic distillation columns with side heat pumps for the propylene/propane separation

J. Rafael Alcántara-Avila [a,*], Fernando I. Gómez-Castro [b], J. Gabriel Segovia-Hernández [b], Ken-Ichiro Sotowa [a], Toshihide Horikawa [a]

[a] Department of Chemical Science and Technology, The University of Tokushima, 2-1 Minami Josanjima-cho, Tokushima 770-8506, Japan
[b] Departamento de Ingeniería Química, Universidad de Guanajuato, Noria Alta s/n, Guanajuato 36050, Mexico

ARTICLE INFO

Article history:
Received 23 December 2013
Received in revised form 23 May 2014
Accepted 14 June 2014
Available online 20 June 2014

Keywords:
Cryogenic distillation
Propylene
Optimization
Heat integration
Refrigeration

ABSTRACT

Propylene is one of the most important products in the petrochemical industry, which is used as raw material for a wide variety of products. The propylene/propane separation is a very energy-intensive process because their boiling points are quite similar. In addition, at atmospheric conditions, their boiling points are −47.6 °C and −42.1 °C, respectively. To separate this mixture conventional columns which operate at high pressure and cryogenic distillation columns which operate at low pressure have been used, however, this approaches are still energy-intensive. This work presents energy-efficient and intensified distillation columns which are adiabatic such as the vapor recompression column (VRC) or diabatic such as columns with heat-integrated stages. A design and optimization procedure, which minimizes the energy consumption in the propylene/propane separation is presented. Conceptual design, superstructure representation, rigorous simulations and mathematical programming techniques are effectively combined to assess all the candidate distillation structures, refrigeration cycles, and heat integration possibilities simultaneously. Results showed that VRC and diabatic distillation columns with heat-integrated stages can reduce the energy consumption between 58 and 75% when compared with conventional distillation at high pressure. Furthermore, the proposed synthesis procedure derived simplified optimal distillation structures with few heat-integrated stages and still attained important energy savings.

1. Introduction

Propylene is used as intermediate in a wide range of chemical processes to produce fibers, foams, plastics, etc. It is mainly obtained as coproduct in the ethylene process and as byproduct in the petroleum refining industry, which in either case, it is mixed with other gases such as hydrogen, ethylene, ethane, propane, etc., but gases lighter than propylene are typically separated at an earlier stage, therefore, propylene is separated from propane in most cases. Since propylene and propane have close boiling points, and are gases at room temperature and atmospheric pressure, its separation is a very energy-intensive process.

Several separation alternatives based on solubility, diffusivity, and molecular size difference have been researched to alleviate the high energy consumption in the propylene–propane separation. Rege and Yang [1] proposed a four-step pressure swing adsorption (PSA) system, which used $AgNO_3/SiO_2$ and AlPO-14 for the separation of propylene from propane at two feed compositions, atmospheric and subatmospheric desorption pressures. Plaza et al. [2] proposed a five-step Vacuum swing adsorption (VSA) system, which used Cu-BTC because of its high pore volume and high sorption capacity, however, the results showed low recovery around 15%. Campo et al. [3] also adopted a five-step VSA system, but using X13 zeolite as sorbent. The results showed high recovery around 75% for their separation. Although membrane-based separations have been also proposed, most of them simultaneously lack high permeability and selectivity, having difficulties in scaling up, and lack of long-term stability due to poisoning of olefin-selective carriers. Pan et al. [4] studied zeolitic imidazolate frameworks for the separation of propylene/propane at several feed composition and temperature conditions. The results showed that the proposed membrane structure exhibited high permeability and selectivity for mixtures rich in propylene at temperatures lower than 22 °C.

Although the aforementioned alternatives can certainly attain energy savings, their capacity and operation time are rather constrained by equipment size and maintenance issues. To satisfy the demand of propylene, distillation is the predominant separation technology to obtain it at large scale. Intensified distillation-based

* Corresponding author. Tel.: +81 886567425; fax: +81 886567425.
E-mail address: alcantara@chem.tokushima-u.ac.jp (J.R. Alcántara-Avila).

http://dx.doi.org/10.1016/j.cep.2014.06.006
0255-2701/

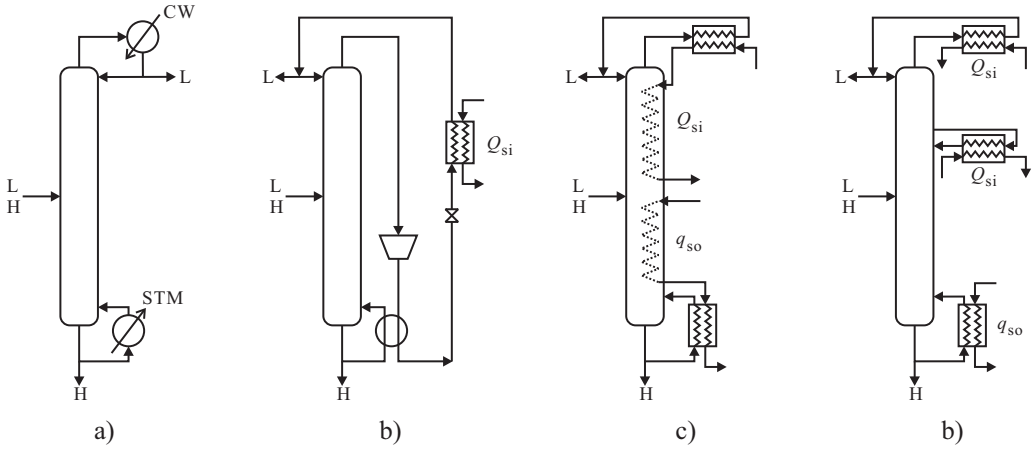

Fig. 1. Candidate distillation structures and heat integration techniques: (a) conventional distillation, (b) vapor recompression column, (c) diabatic distillation, and (d) distillation column with intermediate heat exchangers.

alternatives have been proposed to reduce energy consumption in distillation. Petterson et al. [5] reported profitable membrane-based distillation configurations where a membrane can be located close to the feed stream or at the bottom of the distillation column. Benali and Aydin [6] explored several membrane configurations which could be located at the top, middle and bottom of the distillation column. Their best reported configuration attained economic savings around 36% where one membrane at the top and one at the bottom were installed. Approaches based on mathematical programming have also been proposed [7,8], and they have shown that membrane distillation where the membrane is at an intermediate location can reduce the total annual cost up to 20%. Olujić et al. [9] studied two heat-integrated distillation columns: the vapor recompression column (VRC) and the heat-integrated distillation column (HIDiC). VRC and HIDiC were compared in terms of cost and energy consumption, in which the VRC had higher electricity consumption than the HIDiC, thus higher equipment cost since the compressor cost is predominant in this type of heat-pump assisted distillation structures. In addition, the HIDiC structure exhibited economic and energy savings of 20 and 25%, respectively, over the VRC. Ho et al. [10] presented a dynamic simulation for the HIDiC structure studied by Olujić et al. [9], and they showed that the proposed control configuration can control the HIDiC very well under various disturbances.

Despite of the aforementioned intensified alternatives, the propylene/propane mixture has been conventionally separated by means of distillation columns which operate either at high pressure (e.g., >15 bar) to ensure the use of water as cooling medium or at low temperature (e.g. <5 °C) to use a refrigerant as cooling medium. Regardless of these options, Mauhar et al. [15] have shown that the energy consumption for the separation of propylene and propane is inevitably high if the column operates between 15.95 and 12 bar.

If the separation is carried at low temperature, it is referred to as cryogenic distillation, which requires a refrigerant to provide cooling at a temperature level lower than that at the condenser, thus a distillation column must be coupled with a refrigeration system. However, when refrigerants are used as cooling utilities at the condenser, its temperature range and cost per unit amount of energy exchanged have been set at predefined conditions and treated as parameters in the synthesis problem to derive optimal distillation structures [7,9,10]. This means that the optimization of operating conditions in the refrigeration systems has not been included. In this work the operating conditions of the refrigeration system are optimized simultaneously with the distillation column in order to minimize not only the energy consumption in the latter but also in the former.

Heat integration through intermediate heat exchangers has been reported recently as an alternative to reduce the energy consumption and cost of distillation columns. It has been applied in reactive distillation systems with vapor recompression [11], heat integrated columns for the separation of binary [12,13] and ternary [14] mixtures.

The aim of this work is to propose a systematic procedure to solve the synthesis problem for the separation of the propylene/propane mixture at mild pressure and refrigeration conditions through cryogenic distillation, which embeds a refrigeration system to realize heat integration not only at the condenser or reboiler, but also at several locations in a distillation column. Therefore, the temperature levels of heat sources and heat sinks in the refrigeration system are treated as parameters, and their amount of energy exchanged at any location in the column are treated as optimization variables and embedded in the synthesis problem to find optimal cryogenic distillation columns.

2. Problem statement

Given a liquid mixture of components with low boiling point which is subject to cryogenic distillation, the structure and operating conditions of distillation columns (i.e. process side) as well as the structure and the operating conditions of refrigeration cycles (i.e. refrigeration side) are optimized simultaneously.

Fig. 1 summarizes the distillation columns subject to this research, which comprises conventional distillation columns (CC) in Fig. 1a, VRC in Fig. 1b, diabatic distillation columns (DCC) in Fig. 1c, and distillation columns with heat-integrated stages through the installation of heat pumps (HPC) in Fig. 1d. In DDC all the stages are heat-integrated because heat is supplied or removed in them. In the figure, L denotes the light component, and H the heavy component. CW denotes cooling water and STM steam. q_{so} (Q_{si}) stands for heat source (sink) in the refrigeration side. The arrows without any label entering and leaving heat exchangers denote a heat medium other than cooling water or steam.

Typically in cryogenic distillation, the stages in the column are not heat integrated, thus a refrigeration system is coupled to provide cooling at the condenser, which is at the lowest possible temperature; and to supply heating at the reboiler, which is at the highest possible temperature. Therefore, in the refrigeration side, the temperature difference must be larger than that between condenser and reboiler, which results in a large compressor work duty. Fig. 1c and d exploits the idea of removing heat at locations where the temperature is higher than that at the condenser and supplying it at locations where the temperature is lower than that at the

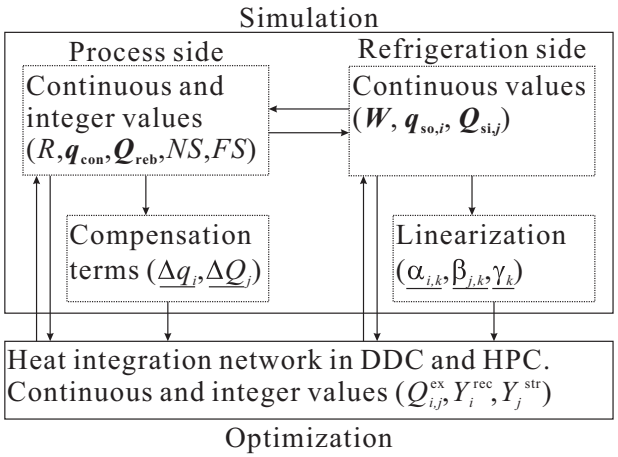

Fig. 2. Simulation-based MILP optimization strategy used in the synthesis problem.

reboiler, thus smaller compressor work duty in the refrigeration side can be realized.

The dotted lines in Fig. 1c represent the energy transfer through all the stages in DCC, and it can be seen that heat exchange is enforced at every stage along the column. HPC differs from DCC because heat integration can be possible at fewer locations and also between non-consecutive stages. Fig. 1d shows one heat exchanger in the rectifying section as a representative example for one possible structure, however, the number of intermediate heat exchangers, the amount of heat exchanged and their locations in the distillation column will be determined through optimization techniques.

The synthesis problem of optimal distillation columns inherently must solve systems of nonlinear and nonconvex equations which combine continuous variables (e.g., reflux ratio, reboiler duty) and discrete variables (e.g., number of stages, feed location). For distillation columns with heat-integrated stages, additional continuous variables (e.g., amount of heat removed or supplied) and discrete variables (e.g., locations subject to heat integration, heat integration network connectivity) must be solved, therefore, optimization approaches must solve complex combinatorial problems and mixed-integer linear programming (MINLP) problems. To avoid such situation, in this work, the process simulator Aspen Plus V7.3.2 is used to solve the nonlinearities and nonconvexities in distillation columns to find continuous variables, and sensitivity analyses are used to find integer variables to optimize CC and VRC. In addition, a mixed-integer linear programming (MILP) problem is formulated to find the best heat integration network and the optimal amount of heat exchanged for DDC and HPC. Fig. 2 shows how simulations and MILP problems are combined to optimize the candidate distillation structures in Fig. 1.

In Fig. 2, the boldfaced variables are the ones obtained from rigorous simulations while the underlined variables can be calculated from linearizations of the boldfaced variables. Thus, they can be entered as parameters in the optimization model. The simulation of the process side and refrigeration side are explained in Sections 3.1 and 3.2, respectively. To derive an MILP problem from nonlinear simulation models, the concept of compensations terms and linearization of the refrigeration side are used and explained in Sections 4.2 and 3.2, respectively. The mathematical formulation of the MILP problem is explained in Section 4.3.

3. Simulation procedure

Conceptual design of distillation columns and refrigeration cycles was carried out and the simulation procedure was executed in Aspen Plus V7.3.2. The following subsections explain the procedure in detail.

3.1. Simulation of distillation columns

Given the feed condition and product specifications, the number of stages in a distillation column can be determined as a function of its operating pressure and reflux conditions. The adopted simulation procedure for CC was:

1. Fix the operating pressure (P), feed, and product specifications.
2. Initialize the parameter ρ, which is the ratio between the minimum reflux ratio (R_{min}) and the actual reflux ratio (R_{act}) given by $R_{act} = \rho R_{min}$ and execute short-cut simulations to calculate the number of stages (NS) and feed stage (FS).
3. Execute rigorous simulations in RADFRAC® for the given conditions in step 1 and the NS and FS obtained in step 2.
4. Obtain the condenser (q_{con}) and reboiler duty (Q_{reb}) from the rigorous simulation results.

Up to step 4, the simulation for CC is completed. The procedure for VRC continues as follows:

5. Drag a pseudo stream that leaves the column from stage 2 as vapor and connect it to the compressor. Then, connect the stream leaving the compressor to the heat exchanger.
6. Set the temperature of the stream leaving the heat exchanger (T_Q^{out}), which must be higher than that of the stream entering the column reboiler (T_{reb}^{in}).
7. Set a new design specification, which satisfies the energy balance $Q_{VR} - Q_{reb} = 0$ by varying the compressor outlet pressure.
8. Calculate the resulting compressor work duty (W_{VR}) and the heat exchanger duty (Q_{VR}).

Up to step 8, the simulation for VRC is completed. However, the stream leaving Q_{VR} becomes a vapor–liquid mixture when depressurized. In such case, a trim condenser is necessary to return this stream to the column as saturated liquid. The trim condenser duty (q_{tri}) can be readily calculated from rigorous simulations when its pressure and vapor fraction are known.

Fig. 3a summarizes the simulation procedure for CC and VRC while Fig. 3b shows the necessary equipment to simulate a VRC structure. In the figure, the dotted lines denote pseudo streams employed for simulating vapor recompression.

3.2. Design of refrigeration cycles

Since refrigeration systems are crucial in cryogenic distillation, their appropriate simulation is important. Fig. 4 shows a conceptual representation of a refrigeration cycle. The working fluid leaves the compressor as a superheated vapor at high pressure and temperature T_0, then it is cooled down to T_1 by removing the heat q_1. This stream can be successively cooled down further to a temperature T_m by removing the heat q_m. Then, the fluid is decompressed by means of a throttling valve. When the pressure drops, the vapor pressure of the fluid decreases, thus it is flashed to a vapor–liquid mixture. It exits the throttling valve at low pressure and temperature t_0, then it is heated up to t_1 by supplying the heat Q_1. This stream can be successively heated up further to a temperature t_n by supplying the heat Q_n. A low pressure stream at temperature t_n is elevated to a higher pressure and temperature T_0 by adding W work duty at the compressor. This closes the refrigeration cycle.

The refrigeration cycle consists of a hot side and a cold side. The hot side comprises streams that are cooled down, thus these streams are regarded as heat sources which can supply heat $q_{so,1}$ through $q_{so,m}$. The cold side comprises streams that are heated up,

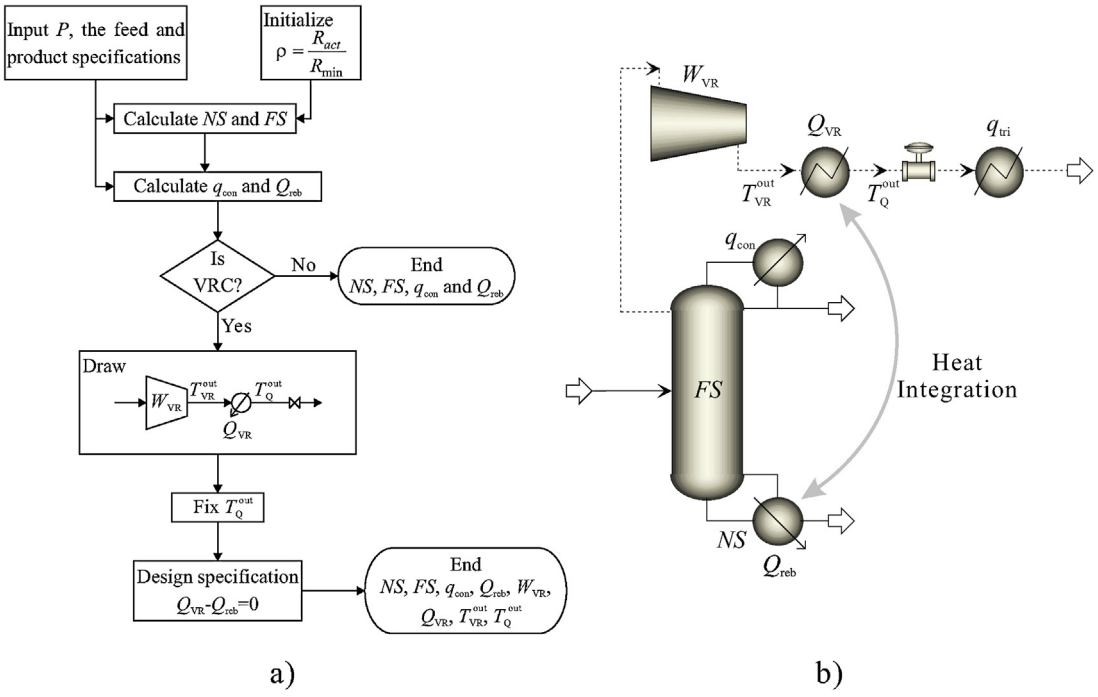

Fig. 3. Simulation procedure for CC and VRC: (a) flowchart, (b) simulation of a VRC structure.

thus these streams are regarded as heat sink which can receive heat $Q_{si,1}$ through $Q_{si,n}$.

The relationship between temperature, pressure and volume for a polytropic process is shown in Eq. (1)

$$\frac{T_{in}}{T_{out}} = \left(\frac{V_{out}}{V_{in}}\right)^{n-1} = \left(\frac{P_{in}}{P_{out}}\right)^{(n-1)/n} \quad (1)$$

where T, V and P denote the temperature, volume and pressure of the working fluid, respectively. The subscripts in and out differentiate the conditions between the compressor inlet and outlet.

For a polytropic compressor, the work duty is calculated by the following equation

$$W = f\Delta h = \frac{P_{in}V_{in}}{\eta_p\left(\frac{n-1}{n}\right)}\left[\left(\frac{P_{out}}{P_{in}}\right)^{(n-1)/n} - 1\right] \quad (2)$$

where W is the compressor work duty, f is the molar flow of the working fluid, and Δh is the enthalpy difference between the stream leaving and entering the compressor. η_p is the compressor polytropic efficiency. Eqs. (1) and (2) are valid for an isentropic compressor if it is assumed that $n = k$, which is the heat capacity ratio C_p/C_v.

The simulation procedure for refrigeration systems was executed as follows:

1. Select a working fluid and its molar flow and inlet temperature (t_n). Then, fix the compressor outlet pressure (P_{out}). At this step, W can be calculated.
2. Insert and connect m heat exchangers in the hot side, and fix their outlet temperature from T_1 to T_m. At this step the heat sources in the hot side, $q_{so,1}$ to $q_{so,m}$, can be calculated.
3. Calculate the pressure after the throttling valve (P_{in}) by fixing the temperature t_0. It can be easily done by setting a design specification.
4. Insert and connect n heat exchangers in the cold side, and fix their outlet temperature from t_1 to t_n. At this step the heat sinks in the cold side, $Q_{si,1}$ to $Q_{si,n}$, can be calculated.

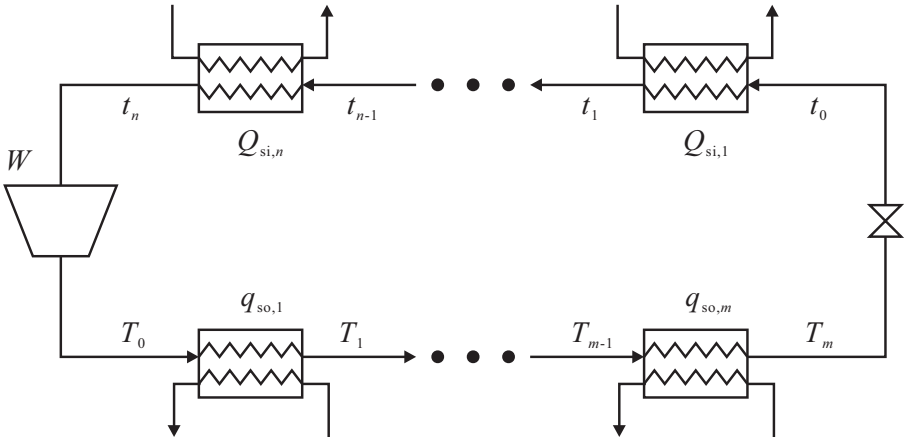

Fig. 4. Conceptual representation of a refrigeration cycle.

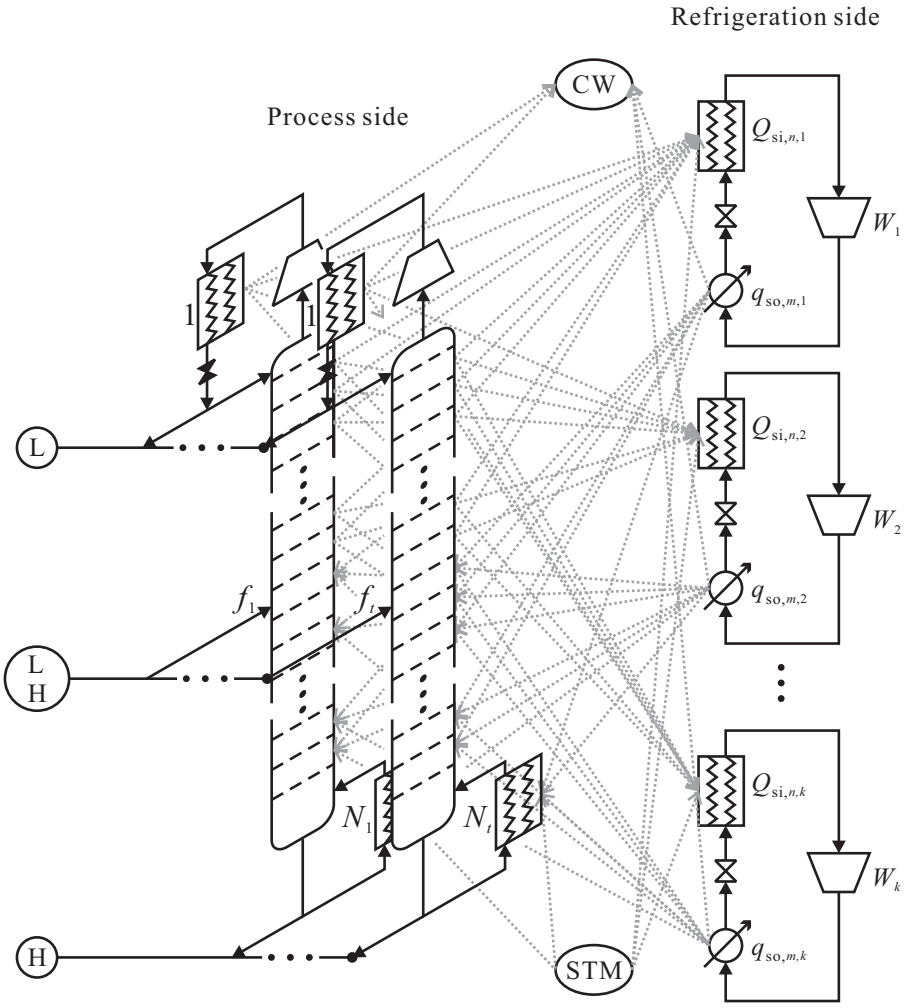

Fig. 5. Superstructure for heat integration between distillation columns and refrigeration cycles.

The relationships between W, $q_{so,m}$, and $Q_{si,n}$ are very important to determine the necessary amount of heat exchanged by the refrigeration cycle.

By adopting the aforementioned procedure, the following linear relations between the compressor work duty and the energy removed or supplied can be derived

$$q_{so,i,k} = \alpha_{i,k} Q_{ref,k} \quad i \in RSO_k, \quad k \in REF \tag{3}$$

$$Q_{si,j,k} = \beta_{j,k} Q_{ref,k} \quad j \in RSI_k, \quad k \in REF \tag{4}$$

$$W_k = \gamma_k Q_{ref,k} \quad k \in REF \tag{5}$$

where $q_{so,i,k}$ denotes the work duty of the i-th heat source in the hot side of a k refrigeration cycle, $Q_{si,j,k}$ denotes the work duty of the j-th heat sink in the cold side of a k refrigeration cycle, and W_k denotes the work duty of a k refrigeration cycle. *REF* is the set of candidate refrigeration cycles, and *RSO* (*RSI*) the set of simulated heat sources (sinks) in the k refrigeration cycles.

Eqs. (3)–(5) define the relations between the amount of energy removed and supplied in the refrigeration system which are represented by the parameters $\alpha_{i,k}$, $\beta_{j,k}$, and γ_k, respectively. The reference exchanger in the refrigeration cycle is the one which operates at the lowest temperature because this is the condition at which refrigeration is available, thus it describes the performance of the refrigeration cycle. Therefore in Fig. 4, $Q_{ref,k} = Q_{si,1,k}$ for each refrigeration cycle k.

4. Synthesis problem

4.1. Superstructure representation

All possible combinations and feasible locations for heat exchange between distillation columns and refrigeration cycles to realize cryogenic distillation can be simultaneously included in the superstructure shown in Fig. 5, which is a state task network representation. The circles represent the states of the original feed and the product specifications. In the process side, each task is a different distillation column at different pressure level and reflux condition with or without vapor recompression. When the compressor work duty, W_{VR}, is zero, the distillation column is regarded as CC, and VRC otherwise. Each distillation column at different pressure and reflux condition is regarded as a different task in the superstructure. In the refrigeration side, each refrigeration cycle represents a different utility where $q_{so,m}$ and $Q_{si,n}$ are regarded as heat sources and heat sinks, respectively, at different temperature levels. Finally, CW and STM provide cooling and heating if necessary to satisfy the energy balance.

4.2. Installation of intermediate heat exchangers

When heat integration takes place at a condenser or reboiler, the reduced energy is equal to the exchanged energy, however, when heat integration takes place in any stage of a column, the reduced energy at a condenser or reboiler is less than the removed

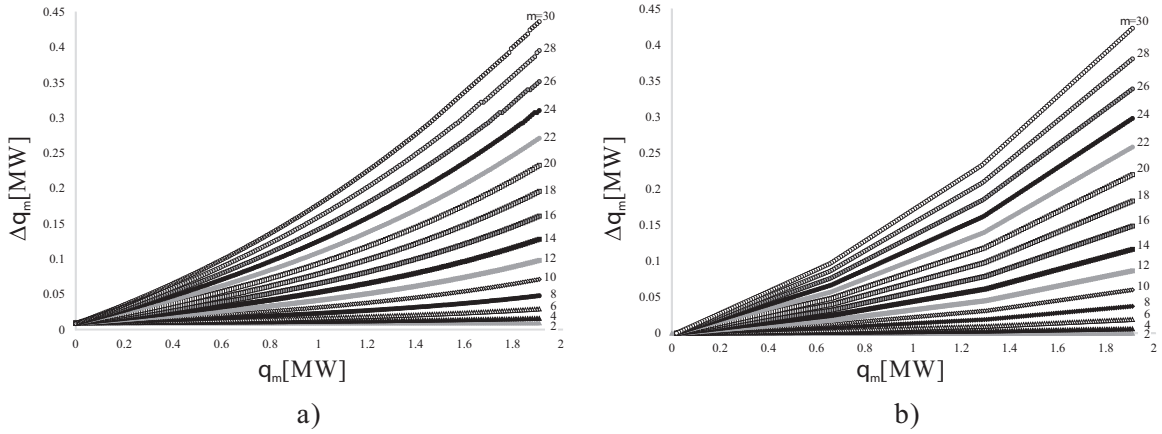

Fig. 6. Condenser compensation terms in the rectifying section: (a) rigorous simulations, (b) piecewise linearization.

or supplied energy in the rectifying or stripping section. Moreover, there are tight and complex relations between the location of heat-integrated stages, the amount of heat removed or supplied, and the resulting condenser and reboiler duty after such heat integration. The calculation of these relations is not trivial and imply the solution of large combinatorial problems between stages in the rectifying section that are heat sources and stages in the stripping section that are heat sinks. One of our previous researches have addressed the aforementioned relations by developing the concept of compensation term [14], in which large values of compensation terms are not desired because they lower the effectiveness of energy reduction at reboilers. Eqs. (6) and (7) show the compensation terms for the rectifying and stripping sections in a distillation column.

$$\Delta q_i = q_i - (q_{\mathrm{con0}} - q_{\mathrm{con}}) \quad i \in REC \tag{6}$$

$$\Delta Q_j = Q_j - (Q_{\mathrm{reb0}} - Q_{\mathrm{reb}}) \quad j \in STR \tag{7}$$

where q_{con0} (Q_{reb0}) is the condenser (reboiler) heat duty prior any heat integration, q_{con} (Q_{reb}) is the condenser (reboiler) heat duty after any heat integration, q_i (Q_j) is the energy removed (supplied) at stage i (j) in the rectifying (stripping) section, and Δq_i (ΔQ_j) is its respective condenser (reboiler) compensation term. *REC* is the set of stages in the rectifying section and *STR* is the set of stages in the stripping section.

Fig. 6a shows the simulation results, which can be obtained through sensitivity analysis by varying q_m at each stage m. They show the relation between the energy supply at a stage m in the rectifying section and its compensation term calculated from Eq. (6). From the simulation results, it can be observed that Δq_m increases steeply as m increases. The data in Fig. 6a from rigorous simulations can be approximated to a set of piecewise linear functions as shown in Fig. 6b, which is divided into 3 segments. By these linearizations, the values of q_{con} can be readily estimated without the need of solving extensive simulations for complex nonlinear combinatorial problems.

4.3. Mathematical formulation for distillation columns with heat-integrated stages

The combination of heat sources and sinks in cryogenic distillation, which is represented by the superstructure in Fig. 5, can be formulated as an optimization problem to derive structures with minimum energy consumption. In addition, if the operating pressure and number of stages are discretized in the process side, the values obtained from Section 3.1 (i.e. q_{con0}, Q_{reb0}, W_{VR}), and the temperature of each stage can be entered as parameters for each task. If the temperature levels of each $q_{\mathrm{so},m}$ and $Q_{\mathrm{si},n}$ in the refrigeration side are also discretized, the values obtained from Section 3.2 (i.e. $\alpha_{i,k}$, $\beta_{j,k}$, γ_k) can be entered as parameters for each refrigeration cycle. Thus, the optimization problem can be formulated by the mixed-integer linear programming (MILP) problem explained in this subsection.

To select one distillation column among all the candidates in the superstructure, an integrality constraint is necessary, and it is represented by

$$\sum_{t \in TK} Z_t = 1 \tag{8}$$

where Z_t is a binary variable assigned to each task in the process side. If a task t is selected, Z_t becomes one, or zero otherwise. *TK* denotes the set of tasks in the process side.

The heat removed from the rectifying section in tasks, and their condenser compensation terms of each stage can be calculated according to

$$\begin{aligned}
&\sum_{j \in RSI_k} Q_{i,j}^{ex} + \sum_{j \in CU} Q_{i,j}^{ex} = q_i \quad i \in REC_t, k \in REF, t \in TK \\
&q_i - Y_i^{\mathrm{rec}} UB \le 0 \quad i \in REC_t, t \in TK \\
&\Delta q_i = \max_s \{a_{i,s} q_i + b_{i,s}\} \quad i \in REC_t, s \in PW, t \in TK \\
&\sum_{i \in REC_t} Y_i^{\mathrm{rec}} - S_{\mathrm{rec}} Z_t \le 0 \quad t \in TK \\
&q_{\mathrm{rec},t} = \sum_{i \in REC_t} q_i \quad t \in TK \\
&\Delta q_{\mathrm{tot},t} = \sum_{i \in REC_t} \Delta q_i \quad t \in TK
\end{aligned} \tag{9}$$

while the heat added to the stripping section, and the reboiler compensation terms of each stage can be calculated according to

$$\begin{aligned}
&\sum_{i \in RSO_k} Q_{i,j}^{ex} + \sum_{i \in HU} Q_{i,j}^{ex} = Q_j \quad j \in STR_t, k \in REF, t \in TK \\
&Q_j - Y_j^{\mathrm{str}} UB \le 0 \quad j \in STR_t, t \in TK \\
&\Delta Q_j = \max_s \{a_{j,s} Q_j + b_{j,s}\} \quad j \in STR_t, s \in PW, t \in TK \\
&\sum_{j \in STR_t} Y_j^{\mathrm{str}} - S_{str} Z_t \le 0 \quad t \in TK \\
&Q_{\mathrm{str},t} = \sum_{j \in STR_t} Q_j \quad t \in TK \\
&\Delta Q_{\mathrm{tot},t} = \sum_{j \in STR_t} \Delta Q_j \quad t \in TK
\end{aligned} \tag{10}$$

where *RSI* (*RSO*) is the set of heat sinks (sources) in the refrigeration side, *CU* (*HU*) is the set of cooling (heating) utilities, and *PW* is the set of segments in the piecewise linearization of the compensation terms. $Q^{ex}_{i,j}$ is the energy exchange between heat sources *SO* ($SO = REC_t \cup RSO_k \cup HU$) and heat sinks *SI* ($SI = STR_t \cup RSI_k \cup CU$) where $t \in TK$ and $k \in REF$. Y^{rec}_i (Y^{str}_j) is the binary variable that becomes one if a heat exchanger is installed at stage i (j) of task t, and zero otherwise. $a_{i,s}$ ($a_{j,s}$) and $b_{i,s}$ ($b_{j,s}$) are the parameters for the piecewise linear functions in segment s for the rectifying (stripping) section. *UB* is the upper bound for heat integration at stages in the rectifying and stripping section. S_{rec} (S_{str}) is the number of stages where heat integration can be enforced for each task. It is worthy to mention that if a task t is not selected, heat integrations at intermediate locations for that task are not allowed. q_{rec} (Q_{str}) is the total amount of energy exchanged through all the stages in the rectifying (stripping) section of a task k. Finally, $\Delta q_{tot,t}$ ($\Delta Q_{tot,t}$) is the overall compensation term in the rectifying (stripping) section of task t. Eqs. (9) and (10) are necessary to estimate the condenser and reboiler duties due to heat integration at stages in all distillation columns.

Eq. (11) shows the Big-M formulation adopted to represent the feasibility criterion for heat integration between heat sources and heat sinks

$$Q^{ex}_{i,j} - FX^{ex}_{i,j} M \le 0 \quad i \in SO, j \in SI$$
$$FX^{ex}_{i,j} = \begin{cases} 1 & \Delta T_{i,j} \ge \Delta T_{min} \\ 0 & \text{otherwise} \end{cases} \quad i \in SO, j \in SI \tag{11}$$

where $FX^{ex}_{i,j}$ is the feasibility matrix for heat integration, M is a big value, $\Delta T_{i,j}$ is the logarithmic mean temperature difference between stages i and j, and ΔT_{min} is the minimum temperature difference to realize heat integration.

The logarithmic mean temperature difference is calculated according to the following equation

$$\Delta T_{i,j} = \begin{cases} \dfrac{(T^{in}_i - t^{out}_j) - (T^{out}_i - t^{in}_j)}{\ln((T^{in}_i - t^{out}_j)/(T^{out}_i - t^{in}_j))} & \text{for } T^{in}_i - t^{out}_j \ge 0 \\ & \text{and } T^{out}_i - t^{in}_j \ge 0 \\ 0 & \text{otherwise} \end{cases} \quad i \in SO, j \in SI \tag{12}$$

where T^{in}_i (T^{out}_i) is the inlet (outlet) temperature of the heat source and t^{in}_j (t^{out}_j) is the inlet (outlet) temperature of the heat sink. $\Delta T_{i,j}$ can only take a positive value if the temperature of the heat source is higher than that of the heat sink.

Eq. (13) shows the energy balance for the condenser and reboiler in the process side

$$q_{rec,t} - \Delta q_{tot,t} = q_{con0,t} Z_t + \Delta Q_{tot,t} \quad t \in TK$$
$$Q_{str,t} - \Delta Q_{tot,t} = Q_{reb0,t} Z_t + \Delta q_{tot,t} \quad t \in TK \tag{13}$$

where the condenser and reboiler duty are multiplied by Z_t, which means splits of the feed and product streams are not allowed.

Eq. (14) shows the energy balance for the heat sources and sinks in the refrigeration side

$$\sum_{j \in STR_t} Q^{ex}_{i,j} + \sum_{j \in RSI_k} Q^{ex}_{i,j} + \sum_{j \in CU} Q^{ex}_{i,j} = q_{so,i,k} \quad i \in RSO_k, k \in REF, t \in TK$$
$$\sum_{i \in REC_t} Q^{ex}_{i,j} + \sum_{i \in RSO_k} Q^{ex}_{i,j} + \sum_{i \in HU} Q^{ex}_{i,j} = Q_{si,j,k} \quad j \in RSI_k, k \in REF, t \in TK \tag{14}$$

Eq. (15) shows the objective function, which minimizes the total energy consumption of steam and electricity in cryogenic distillation columns and refrigeration cycles

$$\min \text{ENERGY} = \sum_{\substack{i \in HU \\ j \in STR_t \\ t \in TK}} Q^{ex}_{i,j} + \sum_{\substack{i \in HU \\ j \in RSI_k \\ k \in REF}} Q^{ex}_{i,j} + \eta \left(\sum_{t \in TK} W_{VR,t} Z_t + \sum_{k \in REF} W_k \right) \tag{15}$$

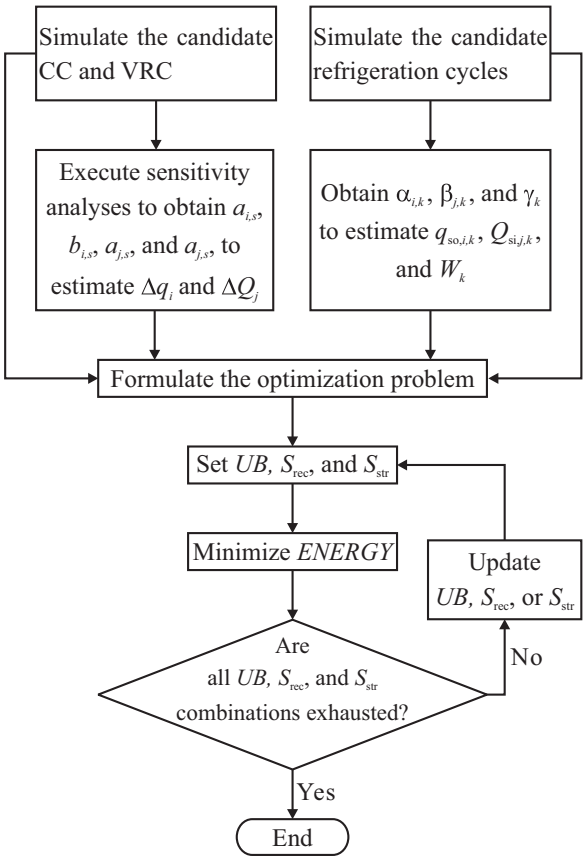

Fig. 7. Flowchart for the proposed synthesis procedure.

where η is a parameter which relates the consumption of primary energy sources per unit amount of electricity generation. In this research, η was equal to 2.73, which is an empirical value used in Japan.

4.4. Synthesis procedure

The synthesis procedure proposed in this research is as follows:

1. Execute the simulation procedures in Section 3 for all the candidate distillation columns and refrigeration cycles.
2. Derive linearizations of condenser and reboiler compensation terms through sensitivity analyses for the simulated distillation column in step 1.
3. Derive linearizations between $q_{so,m}$, $Q_{si,n}$, and W for the simulated refrigeration cycles in step 1.
4. Formulate the optimization problem shown in Section 4.3.
5. Set a value for *UB*, S_{rec}, and S_{str}.
6. Solve the optimization problem to find the best heat integration network between distillation columns and refrigeration cycles.
7. Repeat steps 5 and 6 until the combinations of *UB*, S_{rec}, and S_{str} are exhausted. At this step several optimal solutions are obtained through sensitivity analyses of the parameters *UB*, S_{rec}, and S_{str}.

Fig. 7 summarizes schematically the abovementioned synthesis procedure. Different combinations of *UB*, S_{rec}, and S_{str} will result in several optimal cryogenic distillation structures.

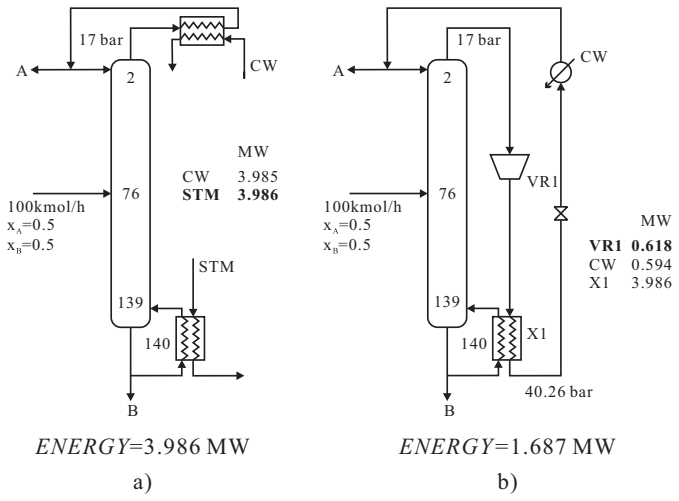

Fig. 8. Results for the propylene/propane separation at high pressure: (a) CC base case, (b) VRC.

5. Results and discussion

5.1. Case study

100 kmol/h of an equimolar propylene/propane mixture which enters as saturated liquid is separated. Propylene is desired with 99.5 mol% purity at the top, and propane with 99.5 mol% purity at the bottom. A pressure drop of 0.69 bar in the distillation columns was assumed. The compressor in the VRC structure and the one in the refrigeration cycles was assumed to be polytropic with an efficiency of 85%. The selected refrigerant was isobutane and the ΔT_{min} was set to 6 °C for heat integration at condensers and reboiles, and 8 °C for heat-integrated stages. In addition, in the refrigeration cycles, the hot side had one heat exchanger and the cold side had two.

Sensitivity analysis for *UB*, S_{rec}, and S_{str} were done to explore several structures with heat-integrated stages and to quantify the trade-off between energy savings and complexity of heat integration networks.

5.2. Simulation results of columns at high pressure

Fig. 8a shows the base CC while Fig. 8b shows the VRC structure which can be easily derived from rigorous simulations. For the sake of comparison, the simulations were done at 17 bar to ensure the use of cooling water. The boldfaced numbers represent the energy input to the distillation column. The VRC can reduce 58% the energy consumption when compared to the base CC, however, it is necessary to recompress the vapor up to 35.34 bar, which leads to severe operating conditions.

To avoid high operating pressure, severe recompression and high reflux ratios, in the next section, distillation columns with side heat pumps, which operate at lower pressure, are presented and their energy savings are assessed in detail.

5.3. Optimization results and sensitivity analysis of structures at low pressure

As the pressure decrease in binary distillation, the reflux ratio and reboiler duty decrease for the same given feed composition and product specifications. However, there are economic limitations and complications in operation because vacuum systems or refrigeration systems will become necessary.

To find the best heat integration network, the MILP problem presented in Section 4.3 was solved in IBM ILOG CPLEX Optimization Studio 12.5. The value for *M* in Eq. (11) was set equal to 20 for the Big-M formulation. The problem included 12 tasks and 50 refrigeration cycles.

Fig. 9 shows optimal solutions for several combinations of *UB*, S_{rec} and S_{str}. It can be observed that the energy consumption decreases as the number of heat integration increases for large values of *UB*, and the energy consumption increases regardless the number of integrations for small values of *UB*. From these results, it is noticed that few heat-integrated stages which can exchange high amount of heat are better than many heat-integrated stages which can exchange small amount of heat. Fig. 9a and b shows the same tendency.

Fig. 9a shows solutions when the number of refrigeration cycles is unconstrained, which means that as many as possible refrigeration cycles can be used. This, however, result in very complex integrations between refrigeration cycles and heat pumps, which may be difficult to realize in practice. To generate less complex integrations, Fig. 9b shows solutions when the number of refrigeration cycles is constrained to a maximum number of 2. The number of refrigeration cycles can be constrained by adding the following equation to the optimization problem.

$$\sum_{k \in REF} Y_k^{ref} \leq 2$$
$$W_k - M Y_k^{ref} \leq 0 \quad k \in REF \tag{16}$$

where Y_k^{ref} is a binary variable which becomes one if a refrigeration cycle is selected and zero otherwise. In Eq. (16), the Big-M formulation is applied to avoid using a compressor if its refrigeration cycle is not selected.

When the number of compressors is unconstrained, the refrigeration side approximates to a reversible process, thus the energy consumption is lower than the constrained case. Nevertheless, the highest absolute and relative gap between the constrained and unconstrained solutions is 0.048 MW and 4.2%, respectively.

Fig. 10 shows several optimal solutions when cryogenic distillation is enforced at 12 bar. Fig. 10a and b shows a CC and VRC structure which uses 2 compressors. In Fig. 10a, X3 exchanges latent heat while X2 exchanges sensible heat. Similarly in Fig. 10b, X1 exchanges latent heat while X2 exchanges sensible heat. At this optimization stage latent and sensible heat transfer are represented separately, but they can be merged into a single heat exchanger at the next design stage. The previous assumption is applied to all the results hereinafter.

Fig. 10c shows a column with 2 heat-integrated stages in the rectifying and stripping section, energy reduction was attained by lowering the reflux ratio, thus increasing the number of stages. In this solution, an outer refrigeration cycle removes (supplies) heat at the condenser (reboiler) while an inner cycle removes (supplies) heat at the stages. Fig. 10d shows a column with 1 heat-integrated stage in the rectifying and stripping section, which lowers the reflux ratio more than Fig. 10c, thus the number of stages increases. In this solution, a refrigeration cycle removes heat in the condenser and the other supplies it to the stages and reboiler.

Fig. 11 shows several optimal solutions when cryogenic distillation is enforced at 9 bar. If the pressure is further reduced, the relative volatility in the propylene/propane mixture increases, thus fewer stages and lower reflux ratio are necessary to attain the same product specifications. Fig. 11a and b shows a CC and VRC structure which uses 2 and 3 compressors, respectively. Fig. 11c shows a column with 1 heat-integrated stage in the rectifying and stripping section, energy reduction was attained by lowering the reflux ratio, thus increasing the number of stages. In this solution, an outer refrigeration cycle removes (supplies) heat at

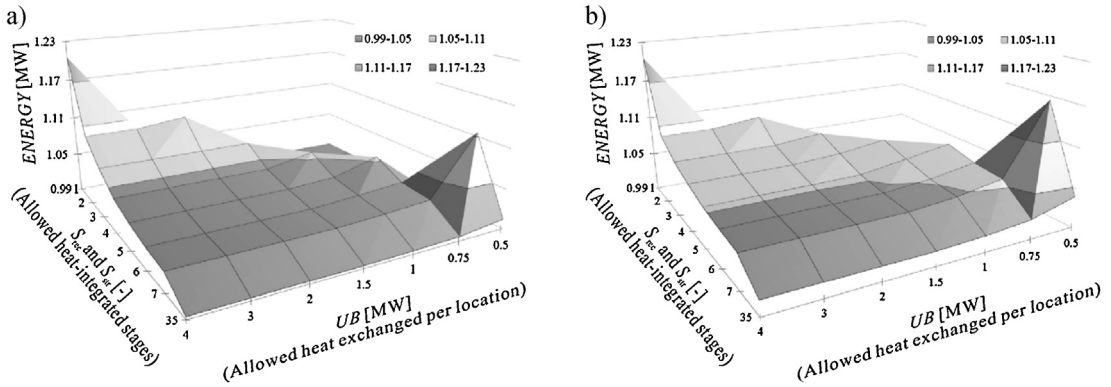

Fig. 9. Optimal distillation columns with heat pumps: (a) unconstrained solution, (b) constrained solution.

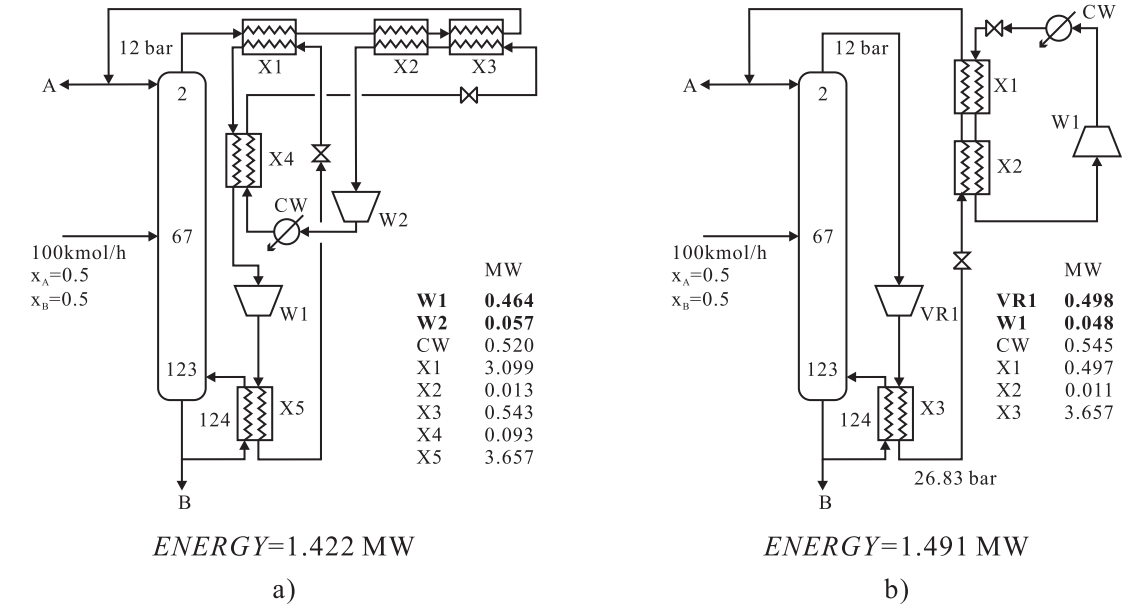

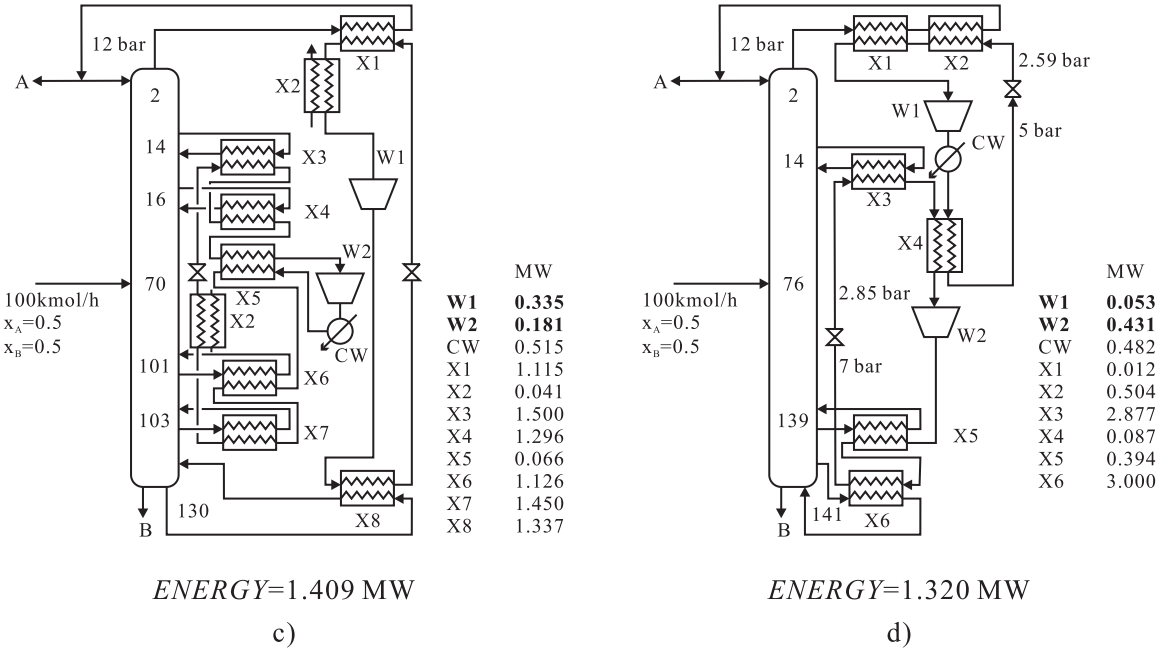

Fig. 10. Optimal distillation columns at 12 bar: (a) CC, (b)VRC, (c) HPC-2, (d) HPC-1.

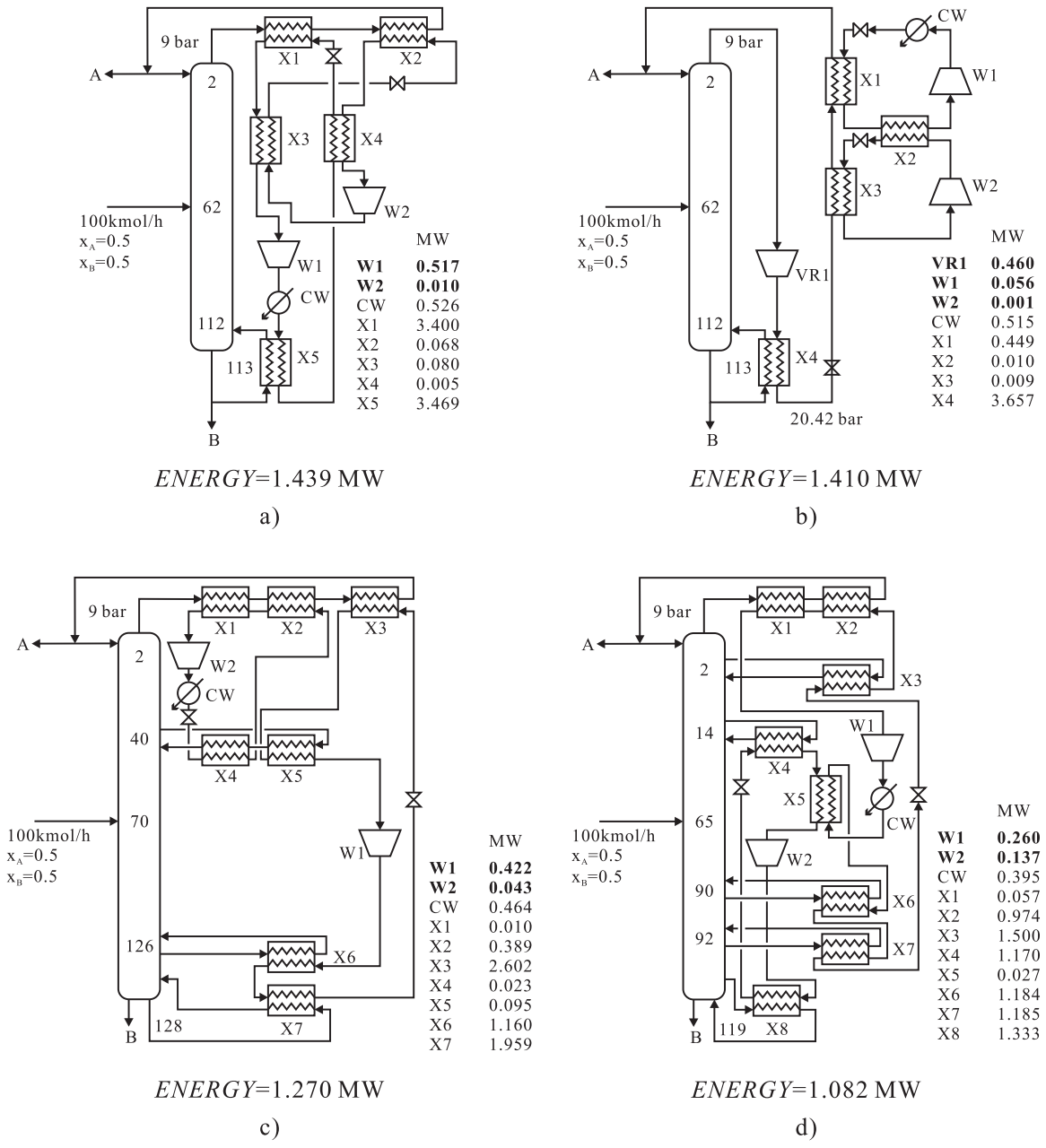

Fig. 11. Optimal distillation columns at 9 bar: (a) CC, (b)VRC, (c) HPC-1, (d) HPC-2.

the condenser (reboiler) while an inner cycle removes heat in the condenser and at stage 40. Fig. 11d shows a column with 2 heat-integrated stages in the rectifying and stripping section. In this solution, a refrigeration cycle removes heat in the condenser and stage 2 and supplies it at stages 90 and 92 while the other refrigeration cycle removes heat at stage 14 and supplies it at the reboiler.

Fig. 12 shows DDC optimal solutions at 12 and 9 bar. In both cases, an outer refrigeration cycle removes (supplies) heat at the condenser (reboiler) while an inner cycle removes (supplies) heat at the stages. Most of the energy is exchanged by the inner refrigeration cycle. In Fig. 12a, heat is removed from stage 14 to 76 and supplied from stage 78 to 109 while in Fig. 12b, heat is removed from stage 14 to 64 and supplied from stage 66 to 98. Although the DDC realizes less energy consumption, a large number of heat exchangers are needed, therefore from the equipment and control point of view, its implementation might be difficult.

From the previous results, it can be shown that energy consumption reduces as the number of heat-integrated stages increases, however, it yields to complex heat integration networks, therefore there is a trade-off between energy savings and complexity in heat integrations, this trade-off can be extended to assess economic aspects and their dynamic performance. From the derived solutions, a set of Pareto optimal solutions can be obtained by fixing the upper bound for heat integration. The lower bound for the Pareto optimal solutions is the DDC in all cases.

While the DDC attained energy savings up to 75% when compared with the base case CC, HPC-1 at 9 bar attained energy savings up to 72.5%, and VRC attained energy savings up to 64.6%. From the presented results, the installation of heat pumps in cryogenic

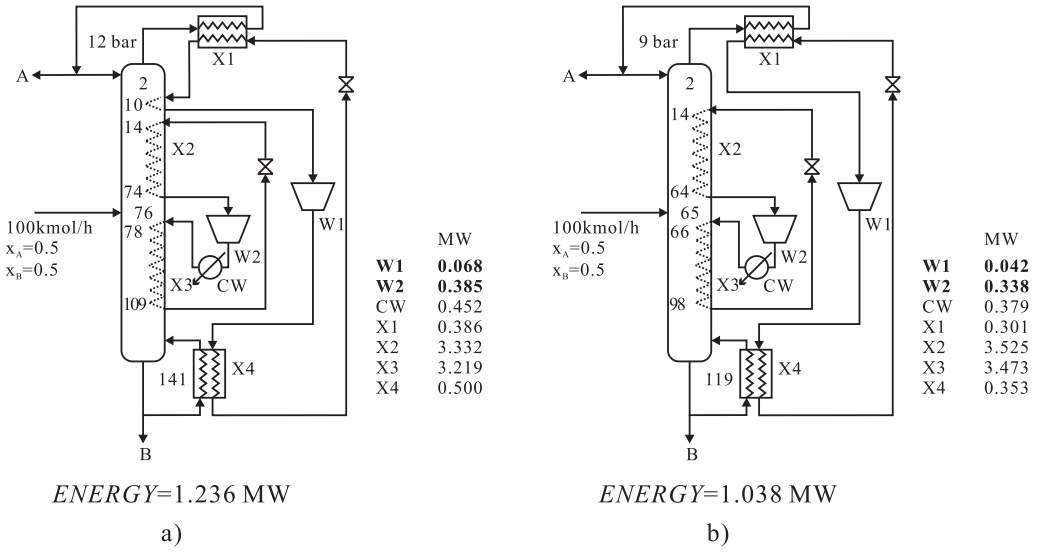

Fig. 12. Optimal DCC: (a) 12 bar, (b) 9 bar.

distillation columns can result in higher energy savings than the typical VRC.

The columns with heat-integrated stages required more stages than the CC and VRC structures to perform the separation. Heat integration at low pressure levels resulted in less reflux ratio, heat duty and compressor work duty. The presented procedure can be extended to other cryogenic systems or any distillation process which can be integrated with one or several refrigeration cycles without loss of generality.

6. Conclusions

This work addressed the problem of cryogenic distillation through a synthesis procedure that combined superstructure formulation, rigorous simulations and optimization techniques. The propylene/propane separation was taken as case study because it is a very energy-intensive process. Distillation columns with and without vapor recompression and several refrigeration cycles were embedded in a superstructure to comprise all the possible heat integrations between refrigeration cycles and any stage in distillation columns. The vapor recompression column was able to reduce the energy consumption by 64.4% while the diabatic distillation column was able to reduce by 75%. Distillation columns with heat-integrated stages were able to reduce the energy consumption between 72.5 and 75%. Thus, all the presented solutions are intensified and energy-efficient alternatives that can reduce the energy consumption in distillation.

Although the diabatic column attained the lowest energy consumption, it resulted in a highly integrated system between the process and refrigeration side. Although the results showed a set of several optimal distillation columns with heat-integrated stages, it was found that few heat-integrated stages which can remove or supply a large amount of energy is more appealing than many heat-integrated stages which can remove or supply a small amount of energy. Most of the optimal solutions had outer and inner refrigeration cycles. While the outer cycle exchanged energy between condenser and reboilers, the inner cycle did it between stages.

In addition, distillation columns with heat-integrated stages require more stages than conventional columns without any integration. It was found that by worsening 8% the energy consumption in the diabatic distillation column, several optimal cryogenic distillation structures with heat-integrated stages can be found with much easier (less integrated) heat integration networks between the process and refrigeration side. The presented synthesis procedure can be extended to any binary and multi-component separation when distillation columns are coupled with refrigeration systems without loss of generality.

Further research about the trade-off between energy consumption, economic assessment and controllability in cryogenic distillation will be conveyed at a later stage.

References

[1] S.U. Rege, R.T. Yang, Propane-propylene separation by pressure swing adsorption: sorbent comparison and multiplicity of cyclic steady states, Chem. Eng. Sci. 57 (2002) 1139–1149.
[2] M.G. Plaza, A.M. Ribeiro, A. Ferreira, J.C. Santos, U.-H. Lee, J.-S. Chang, J.M. Loureiro, A.E. Rodrigues, Propylene/propane separation by vacuum swing adsorption using Cu-BTC spheres, Sep. Purif. Technol. 90 (2012) 109–119.
[3] M.C. Campo, A.M. Ribeiro, A. Ferreira, J.C. Santos, C. Lutz, J.M. Loureiro, A.E. Rodrigues, New 13X zeolite for propylene/propane separation by vacuum swing adsorption, Sep. Purif. Technol. 103 (2013) 60–70.
[4] Y. Pan, T. Li, G. Lestari, Z. Lai, Effective separation of propylene/propane binary mixtures by ZIF-8 membranes, J. Membr. Sci. 390–391 (2012) 93–98.
[5] T. Petterson, A. Argo, R.D. Noble, C.A. Kova, Design of combined membrane and distillation processes, Sep. Technol. 6 (1996) 175–187.
[6] M. Benali, B. Aydin, Ethane/ethylene and propane/propylene separation in hybrid membrane distillation systems: optimization and economic analysis, Sep. Purif. Technol. 73 (2010) 377–390.
[7] J.A. Caballero, I.E. Grossmann, M. Keyvani, E.S. Lenz, Design of hybrid distillation-vapor membrane separation systems, Ind. Eng. Chem. Res. 48 (2009) 9151–9162.
[8] I.K. Kookos, Optimal design of membrane/distillation column hybrid processes, Ind. Eng. Chem. Res. 42 (2003) 1731–1738.
[9] Ž. Olujić, L. Sun, A. de Rijke, P.J. Jansens, Conceptual design of an internally heat integrated propylene–propane splitter, Energy 31 (2006) 3083–3096.
[10] T.-S. Ho, C.-T. Huang, J.-M. Lin, L.-S. Lee, Dynamic simulation for internally heat-integrated distillation columns (HIDiC) for propylene–propane system, Comput. Chem. Eng. 33 (2009) 1187–1201.
[11] V. Kumar, B. Kiran, A.K. Jana, A.N. Samanta, A novel multistage vapor recompression reactive distillation system with intermediate reboilers, AIChE J. 59 (3) (2013) 761–771.
[12] D. Chen, X. Yuan, L. Xu, K.T. Yu, Comparison between different configurations of internally and externally heat-integrated distillation by numerical simulation, Ind. Eng. Chem. Res. 52 (2013) 5781–5790.
[13] Y. Wang, K. Huang, S. Wang, A simplified scheme of externally heat-integrated double distillation columns (EHIDDiC) with three external heat exchangers, Ind. Eng. Chem. Res. 49 (2010) 3349–3364.
[14] J.R. Alcántara-Avila, M. Kano, S. Hasebe, New synthesis procedure to find the optimal distillation sequence with internal and external heat integrations, Ind. Eng. Chem. Res. 52 (2013) 4851–4862.
[15] S.M. Mauhar, B.G. Barjaktarović, M.N. Sovilj, Optimization of propylene–propane distillation process, Chem. Pap. 58 (6) (2004) 386–390.